Monte Carlo simulation to investigate the formation of molecular hydrogen and its deuterated forms

Dipen Sahu [a], Ankan Das [a,*], Liton Majumdar [a], Sandip K. Chakrabarti [b,a]

[a] Indian Centre For Space Physics, 43 Chalantika, Garia Station Road, Kolkata 700084, India
[b] S.N. Bose National Center for Basic Sciences, JD-Block, Salt Lake, Kolkata 700098, India

HIGHLIGHTS

- Monte Carlo simulation was conducted to investigate the formation of H_2, HD & D_2.
- A scaling factor (S_f) was defined to correlate the rate equation & Monte Carlo method.
- The parameter β (catalytic capacity) was defined to study the recombination efficiency.
- The initial D/H ratio was varied to determine the deuterium fractionation of H_2.

ABSTRACT

H_2 is the most abundant interstellar species, and its deuterated forms (HD and D_2) are also present in high abundance. The high abundance of these molecules could be explained by considering the chemistry that occurs on interstellar dust. Because of its simplicity, the rate equation method is widely used to study the formation of grain-surface species. However, because the recombination efficiency for the formation of any surface species is highly dependent on various physical and chemical parameters, the Monte Carlo method is best suited for addressing the randomness of the processes. We perform Monte Carlo simulations to study the formation of H_2, HD and D_2 on interstellar ice. The adsorption energies of surface species are the key inputs for the formation of any species on interstellar dusts, but the binding energies of deuterated species have yet to be determined with certainty. A zero-point energy correction exists between hydrogenated and deuterated species, which should be considered during modeling of the chemistry on interstellar dusts. Following some previous studies, we consider various sets of adsorption energies to investigate the formation of these species under diverse physical conditions. As expected, notable differences in these two approaches (rate equation method and Monte Carlo method) are observed for the production of these simple molecules on interstellar ice. We introduce two factors, namely, S_f and β, to explain these discrepancies: S_f is a scaling factor, which can be used to correlate the discrepancies between the rate equation and Monte Carlo methods, and β indicates the formation efficiency under various conditions. Higher values of β indicate a lower production efficiency. We observed that β increases with a decrease in the rate of accretion from the gas phase to the grain phase.

Keywords:
Astrochemistry
Molecular cloud
ISM: molecules
ISM: abundances

1. Introduction

Molecular hydrogen is the most abundant and simplest species in the interstellar medium (ISM). Indeed, H_2 is the most important molecule because it is the first and most important precursor for creating other complex molecules. Simpler molecules are formed primarily on grain surfaces and then desorbed to the gas phase (Gould and Salpeter, 1963). The importance of grain chemistry has previously been described in the literature (Hasegawa et al., 1992; Chakrabarti et al., 2006a,b; Cuppen and Herbst, 2007; Das et al., 2008a,b, 2010, 2013a,b; Das and Chakrabarti, 2011; Majumdar et al., 2012, 2013; Das et al., 2015; Sivaraman et al., 2014). Even without explicit grain chemistry, effective rates have occasionally been used in studying the formation of bio-molecules (Chakrabarti and Chakrabarti, 2000a,b) For large grains or high accretion rates, the rate equation method (Biham et al., 2001) can be used to explain the abundances of surface species. However, due to the inherent randomness of the processes, particularly

* Corresponding author.
E-mail addresses: dipenthink@gmail.com (D. Sahu), ankan.das@gmail.com (A. Das), liton@csp.res.in (L. Majumdar), chakraba@bose.res.in (S.K. Chakrabarti).

when the grain size is small and/or the accretion rate is small, the simple rate equation method is not sufficient for explaining the recombination efficiency of interstellar surface species. It is thus essential to consider the Monte Carlo method to account for all of the features.

Despite the low elemental abundance of atomic deuterium (a D/H ratio of $\sim 10^{-5}$ according to Linsky et al. (1995)), several complex molecules have been found to be heavily fractionated (Majumdar et al., 2014a,b) in the ISM. Similar to normal hydrogen molecules, the deuterated forms of hydrogen can also be synthesized on interstellar grains. Chakrabarti et al. (2006a,b) conducted Monte Carlo simulations to determine the exact recombination efficiency for the formation of H_2. Following a similar approach, in this work, we use both the rate equation method and the Monte Carlo method to investigate the various aspects involved during the formation of H_2, HD and D_2.

The remainder of this paper is organized as follows. In Section 2, the computational details are presented. The implications of the results are discussed in Section 3. Finally, in Section 4, we draw our conclusions.

2. Computational details

2.1. Rate equation method

A small chemical network that contains H and D is used here. At any time t, let N_x be the number of species x on a grain that possesses S number of adsorption sites. Then, the governing equations for all surface species in our network can be written as follows:

$$\frac{dN_H}{dt} = F_H - W_H N_H - 2a_H N_H^2/S - a_{HD} N_H N_D/S, \tag{1}$$

$$\frac{dN_{H_2}}{dt} = F_{H_2} + \mu_{H_2} a_H N_H^2/S - W_{H_2} N_{H_2}, \tag{2}$$

$$\frac{dN_{D_2}}{dt} = F_{D_2} + \mu_{D_2} a_D N_D^2/S - W_{D_2} N_{D_2}, \tag{3}$$

$$\frac{dN_D}{dt} = F_D - W_D N_D - 2a_D N_D^2/S - a_{HD} N_H N_D/S, \tag{4}$$

$$\frac{dN_{HD}}{dt} = F_{HD} + \mu_{HD} a_{HD} N_H N_D/S - W_{HD} N_{HD}, \tag{5}$$

where F_x, a_x and W_x represent the accretion, hopping and desorption rates, respectively, for species x in units of sec^{-1}. μ_x represents a spontaneous desorption factor. It is assumed that $(1-\mu_x)$ factor of xth species could enter the gas phase immediately after its formation on a grain. From the experimental results of Katz et al. (1999), we use $\mu_{H_2} = 0.33$ for olivine grains and $\mu_{H_2} = 0.413$ for amorphous carbon grains. We also use a similar spontaneous desorption factor for HD and D_2. The accretion rate (F_x) of the xth species is calculated from

$$F_x = t_x A \langle V \rangle N_x, \tag{6}$$

where t_x is the sticking coefficient, A is the surface area of the grain in units of cm^2, $\langle V \rangle$ is the average thermal velocity $\left(\langle V \rangle = \sqrt{\frac{8kT}{m\pi}}\,\mathrm{cm\,sec^{-1}}\right)$, and n_x is the gas phase concentration of the xth species (in cm^{-3}).

2.1.1. Sticking coefficient

Because the sticking coefficient of H_2 is ~ 0 at $T = 10$ K (Leith-Devlin et al., 1985), we consider the sticking coefficients (t_x) of H_2, HD and D_2 to be ~ 0 in this work. Thus, from Eq. (6), we have F_{H_2}, F_{HD} & $F_{D_2} = 0$. In reality, the sticking probability of a species is primarily governed by the kinetic energy of the incoming species and the adsorption energy of that species with the grain surface. Because hydrogen is the lightest species, the hydrogenation reaction is the fastest reaction on the grain surface. Various attempts have been made over the past few decades to determine the sticking coefficient. Buch and Zhang (1991) performed molecular dynamics simulations to numerically evaluate the sticking of hydrogen atoms with clusters of water molecules. According to their study, the sticking coefficient depends on the following:

$$S = (K_B T/E_0 + 1)^{-2}, \tag{7}$$

where $E_0/K_B = 102$ K for H atoms and 200 K for D atoms. According to Chaabouni et al. (2012), a sticking parameter of $\sqrt{10/T}$ could be adopted. Recently, Matar et al. (2010) performed an experiment to model the sticking parameters of H_2 and D_2 and their dependence on the impinging molecular beam temperature. They determined an analytical formula (Eq. (8)) for describing the sticking coefficient at any temperature T. From the outcome of their experiments and the interpretation of Chaabouni et al. (2012), the sticking coefficient can be parameterized for hydrogen and deuterium on silicate surfaces under interstellar conditions. They noted that the sticking coefficients of these species with silicate grains behave in the same manner as they would on icy dust grains. Their prescribed variation of the sticking parameter is as follows:

$$S(T) = S_0 \frac{(1 + \beta T/T_0)}{(1 + T/T_0)^{\sigma}}, \tag{8}$$

where S_0 is the sticking coefficient of particles at zero temperature and T_0 is a critical temperature obtainable using experimental data. σ defines the geometry of the incident beam. In our simulation, unless otherwise stated, we always consider the sticking coefficient of all the species to be 1. For a special case, we consider the assumption of Chaabouni et al. (2012).

2.1.2. Accretion, diffusion and desorption

The effective accretion rate on a typical grain is defined as $\phi_x = F_x\left(1 - \Sigma_i f_{gr_{xi}}\right)$, where $\Sigma_i f_{gr_{xi}}$ is the fraction of the grain that could be occupied by x_i number of species. The hopping rate of a species x is calculated as

$$a_x = \nu_x \exp^{-E_{bx}/K_b T}, \tag{9}$$

where ν_x is the vibrational frequency and E_{bx} is the energy barrier for diffusion. The vibrational frequency of any species x is calculated as

$$\nu_x = \sqrt{\frac{2sE_{dx}}{\pi^2 m_x}}, \tag{10}$$

where m_x is the mass of species x, E_d is the adsorption energy of species x, and s is the surface density of sites in units of cm^{-2} ($s = 10^{14}\,cm^{-2}$ is used). Finally, the desorption rate of species x is calculated as

$$W_x = \nu_x \exp\left(-E_{bx}/K_b T\right). \tag{11}$$

2.1.3. Binding energies

Binding energies are important for determining the mobility of surface species. From the experimental findings of Pirronello et al. (1997, 1999), Katz et al. (1999) concluded that atomic hydrogen moves considerably more slowly than what is generally used in various simulations. In our simulation, we use these experimental findings. In Katz et al. (1999), E_b and E_d were obtained for H atoms. However, for H_2 molecules, only E_d was defined. Because interactions between adsorbed H and D atoms and grains are different, a zero-point energy correction due to isotopic effects should be considered because the binding energies of deuterated species

must be different. Because a D atom is heavier than a H atom, it would sit at a level lower than H in any potential surface if zero-point energy is included (Lipshtat et al., 2004). Caselli et al. (2002) proposed a difference of 2 meV between desorption energies and barriers against diffusion. Following this assumption, Lipshtat et al. (2004) (hereafter LBH) considered a 2 meV energy difference between H and D atoms for barriers against diffusion. They considered the energy barrier against diffusion for H atoms to be 35 meV, whereas for D atoms, they considered it to be 37 meV. Regarding desorption energies, they considered the desorption energy to be 50 meV for H atoms and 60 meV for D atoms. Therefore, regarding the barrier against desorption, LBH considered an energy difference of 10 meV. Following LBH, this larger difference for desorption was considered because the barrier against diffusion balances the zero-point energy of a potential well with that of a saddle point, while desorption does not possess a saddle point.

Due to the lack of a consensus on binding energies, we use three sets of energy barriers in our simulations. These sets are shown in Table 1. The first set corresponds to experimental binding energies, which were taken from Katz et al. (1999) for olivine grains. The second set corresponds to experimental values obtained for amorphous carbon grains (Katz et al., 1999), and the third set is the same as that used by LBH. The binding energies for deuterated species are calculated using the following scaling relations:

$$E_b(D) = E_b(H) \times \frac{37\ (E_b(D)\ \textit{from LBH})}{35\ (E_b(H)\ \textit{from LBH})},$$

$$E_d(D) = E_d(H) \times \frac{60\ (E_d(D)\ \textit{from LBH})}{50\ (E_d(H)\ \textit{from LBH})},$$

$$E_d(HD, D_2) = E_d(D) \times \frac{46.7\ (E_d(H_2)\ \textit{for amorphous carbon from Katz et al.}\ (1999))}{56.7\ (E_d(H)\ \textit{for amorphous carbon from Katz et al.}\ (1999))}.$$

Following Hasegawa et al. (1992) and Das et al. (2008a) and the references therein, we consider $E_d(x) = 0.3\,E_b(x)$ for H_2, HD and D_2 molecules. In the case of set 3, the desorption energy for H_2 was not available. We use the following relation to compute the desorption energy of H_2 for set 3:

$$E_d(H_2) = E_d(H) \times \frac{46.7\ (E_d(H_2)\ \textit{for amorphous carbon from Katz et al.}\ (1999))}{56.7\ (E_d(H)\ \textit{for amorphous carbon from Katz et al.}\ (1999))}.$$

In reality, the nature of the grain surface is not always simple. There might be various types of lattice defects and various phases. Defects with enhanced binding energies (Hollenbach et al., 1971) could allow for the formation of H_2 up to 50 K. In our simulation, we do not consider such types of grains and use a very low temperature window (8–25 K).

2.2. Procedures adopted in the Monte Carlo simulation

To preserve randomness in the molecular formation process, it is essential to develop a Monte Carlo algorithm to mimic an exact scenario. The formation of molecules on grains is primarily due to two types of forces, namely, (i) weak van der Waals interactions and (ii) strong covalent bonding (chemisorption). For the low-temperature region and/or for low surface temperatures, atoms are weakly bound to surfaces via the first type of force, which is called physisorption. Here, the energy is on the order of a few meV. Because species are weakly bound to surfaces, they can move around the surfaces via quantum mechanical tunneling or through thermal hopping. These processes are completely random. A species can move in any direction on the grain surface and can combine with another species to form a third species. We assume the surface to be a square lattice that contains $n \times n$ number of sites in each direction. To mimic the spherical nature of the grain, we consider periodic boundary conditions. Simulations on a complex-shaped grain are outside the scope of the present work and will be addressed in future work.

The governing equations (Eqs. (1)–(5)) are implemented in the Monte Carlo method by assuming a four-step process. The first step is accretion of a gas phase species onto a grain surface. The second step is diffusion of the surface species. The third step is reaction among hopping species (i.e., at chance-meeting sites). Finally, the fourth step is evaporation of the product to the gas phase. The reaction could occur via thermal diffusion or quantum mechanical tunneling. Because we are considering experimental values of binding energies, only thermal hopping is considered. The production of surface species via the Eley–Rideal mechanism (Das et al., 2008a and references therein) is also considered. All the possibilities in the Monte Carlo method are handled by generating random numbers as and when required.

In our simulation, the smallest time scale is the hopping time scale of H or D atoms. The accretion time scale is considerably longer than the hopping time scale. Therefore, for simplicity, we drop a hydrogen atom after every a_H/F_H steps and a deuterium atom after every a_D/F_D steps. The dropping locations are automatically chosen by generating a pair of random numbers. Depending on the number (n) of sites in each direction of the considered grain, the random numbers are scaled. While dropping H or D, if the designated location is already occupied by H_2, HD or D_2, then we search for a different site for its landing. However, if the site is occupied by D or H, then HD/D_2 or H_2/HD could be formed. Depending on the binding energies, surface species are allowed to hop in any of the four directions. The directions are selected by generating random numbers. When an atom meets another atom via thermal hopping, a new species could be formed with certainty (i.e., no activation barrier is considered). The evaporation of surface species is also handled by generating random numbers. The desorption rate for any surface species is calculated using Eq. (9), which implies that species x will leave after $1/W_x$ s. We generate random numbers after every $1/a_H$ s to check this desorption probability. If this number is less than W_x/a_x, then selected x species are

Table 1
Binding energies used in our simulations.

Species	Olivine grain (set 1)		Amorphous carbon grain (set 2)		Lipshtat et al. (2004) (set 3)	
	E_b (in meV)	E_d (in meV)	E_b (in meV)	E_d (in meV)	E_b (in meV)	E_d (in meV)
H	24.7	32.1	44.0	56.7	35.0	50.0
D	26.1	38.5	46.5	68.0	37.0	60.0
H_2	8.1	27.1	14.0	46.7	12.4	41.2
HD	9.8	32.5	16.8	56.0	14.8	49.4
D_2	9.8	32.5	16.8	56.0	14.8	49.4

released from the grain phase. There is another type of desorption, namely, spontaneous desorption, which is also handled by generating random numbers. This desorption term determines whether any newly formed species will remain on the grain surface or desorb from the surface.

3. Results and discussions

Fig. 1 presents the chemical evolution of the surface species (H, H_2, D, HD & D_2). The results from both the rate equation method and the Monte Carlo method are shown. Clear differences between these two methods are visible. Here, we consider amorphous carbon grains with a hydrogen (atomic form) number density $n_H = 10^2$ cm^{-3}, $T = 15$ K and initial atomic D/H ratio (hereafter r_D) = 0.1. The surface abundance of H atoms achieved a steady state after $\sim 10^5$ s, whereas for D atoms, steady state is achieved after $\sim 10^6$ s. For this set of physical parameters, HD is the most abundant species on the grain surface. A steady state would be achieved beyond 2×10^7 s. Note that for this choice of physical parameters, HD and D_2 are overproduced in the rate equation method (Fig. 1).

Fig. 2 presents the efficiency windows for the formation of H_2, D_2 and HD molecules for olivine grains (Fig. 2a), amorphous carbon grains (Fig. 2b) and a type of grain with binding energies in between those of olivine and amorphous carbon (Fig. 2c, with set 3 energy values of Table 1) (Fig. 2c) for $n_H = 10^2$ cm^{-3} and $r_D = 0.1$. The production efficiency is defined by the following relation:

$$\eta_{H_2} = \frac{2R_{H_2}}{F_H}, \tag{12}$$

$$\eta_{D_2} = \frac{2R_{D_2}}{F_D}, \tag{13}$$

$$\eta_{HD} = \frac{R_{HD}}{F_H + F_D}, \tag{14}$$

where R_{H_2}, R_{D_2} and R_{HD} are the gas phase productions of H_2, D_2 and HD, respectively. The gas phase production of these species solely depends on the barrier against desorption (i.e., thermal desorption). Thus,

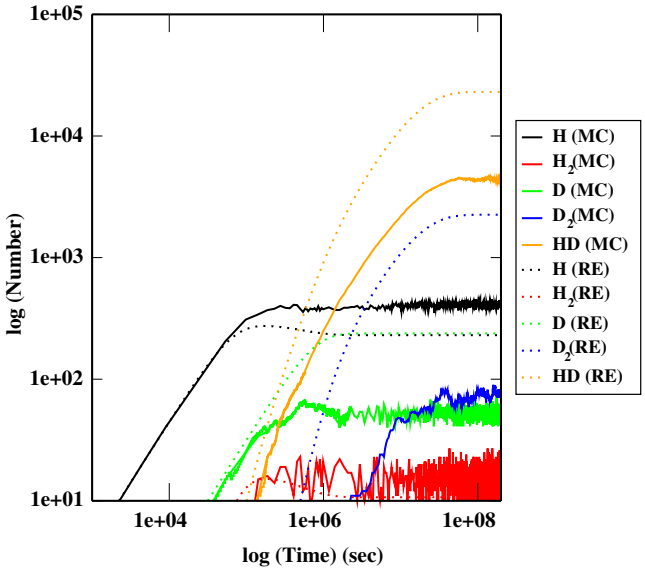

Fig. 1. Time evolution of the abundances of H, H_2, D, HD & D_2 according to the rate equation method (dotted lines) and Monte Carlo method (solid lines). Simulations were performed for an amorphous carbon grain maintained at 15 K, $n_H = 10^2$ cm^{-3} and $r_D = 0.1$.

$$R_{H_2} = W_{H_2} N_{H_2},$$

$$R_{D_2} = W_{D_2} N_{D_2},$$

$$R_{HD} = W_{HD} N_{HD}.$$

As shown in Fig. 2, distinct features are observed for various isotopes of H_2. Solid lines represent the results obtained using the Monte Carlo method, whereas dotted lines represent the results obtained using the rate equation method. The difference between these two methods could be understood from Fig. 2. The Monte Carlo method provides exact production rates due to the consideration of randomness. Here, we are computing the efficiency by considering the average production during the last few seconds. We find an interesting feature in the results of the Monte Carlo method (Fig. 2a–c). We observe a dip in the efficiency profile of HD at the location where the efficiency profile of D_2 contains a peak. This feature is prominent in case of the olivine grain (Fig. 2a). A decreasing feature in the efficiency profile of HD is visible at $T = 11.5$ K (Fig. 2a), whereas at the same location, the maximum efficiency is obtained for D_2. This result indicates that, due to efficient production of D_2, some D atoms are consumed, which in turn decreases the production efficiency of HD. In Fig. 2b and c, this feature is not pronounced due to the lower production of D_2.

In all cases, the rate equation method shows a lower efficiency (under production) for the production of H_2 but a higher efficiency (over production) in the case of HD and D_2. In this context, we can compare Figs. 1 and 2b because, in both cases, we use amorphous carbon grains. Fig. 2b shows that the production efficiencies of HD and D_2 are higher in the case of the rate equation method, which justifies the over production of HD and D_2 in the rate equation method (Fig. 1). Because the Monte Carlo method is more accurate, we recommend that this method be used for all surface reactions. In the case of olivine grains, the efficiency window for H_2 is wider and extends from 8 K to 10 K. For HD, this window ranges from 9–14 K. For D_2, the window is very narrow, and a peak is obtained at approximately 11.5 K. For amorphous carbon grains (Fig. 2b), this window is 11–16, 15–19, and 21–22 K for H_2, D_2 and HD, respectively. As shown in Fig. 2c, the efficiency windows are 11–16, 14–19 and 14–17 K for H_2, D_2 and HD, respectively.

Thus far, we have discussed the gas phase abundances of various isotopes of hydrogen molecules by considering thermal desorption from interstellar grains only. However, there should be another probability of desorption by which the gas phase would be populated. This is called the spontaneous desorption process, in which some fraction of species could be evaporated immediately after their formation. This process occurs due to the energy liberated during some reactions. To account for this feature in our model, we consider that a factor $(1 - \mu)$ of N_{H_2}, N_{D_2} and N_{HD} is lost to the gas phase. According to Katz et al. (1999), for an olivine grain, $\mu_{H_2} = 0.33$ may be used, and for an amorphous carbon grain, $\mu_{H_2} = 0.413$ could be used. Due to the lack of experimental data, we use the same μ values for HD and D_2 ($\mu_{H_2} = \mu_{D_2} = \mu_{HD}$). Furthermore, random numbers are generated for each newly formed H_2, D_2 and HD, and a fraction of species are allowed to populate the gas phase upon their production. In Fig. 3, we compare the efficiency windows of H_2, D_2 and HD by considering the with (dashed line) and without (solid line) spontaneous desorption term. Here, we consider $n_H = 10^2$ cm^{-3} and $r_D = 0.1$ for the olivine grain. When spontaneous desorptions are allowed, molecules begin to efficiently produce in the gas phase at somewhat lower temperatures. For example, the production efficiency of H_2 attains a peak value at 8 K when the spontaneous desorption term is not considered (solid line in Fig. 3). With the spontaneous desorption factor (dashed line in Fig. 3), the peak value for the production efficiency of H_2 occurs at 7.5 K. For HD, the solid line (no desorption) in Fig. 3

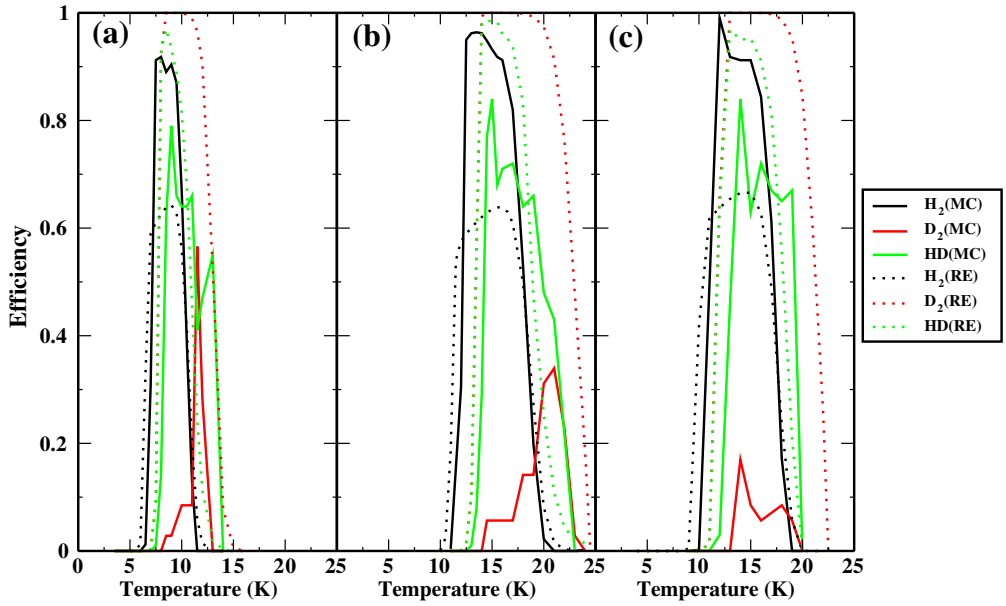

Fig. 2. Efficiency windows for various sets of binding energies for (a) olivine, (b) amorphous carbon and (c) the LBH case. Solid lines are the results obtained using the Monte Carlo method, and dotted lines are the results obtained using the rate equation method.

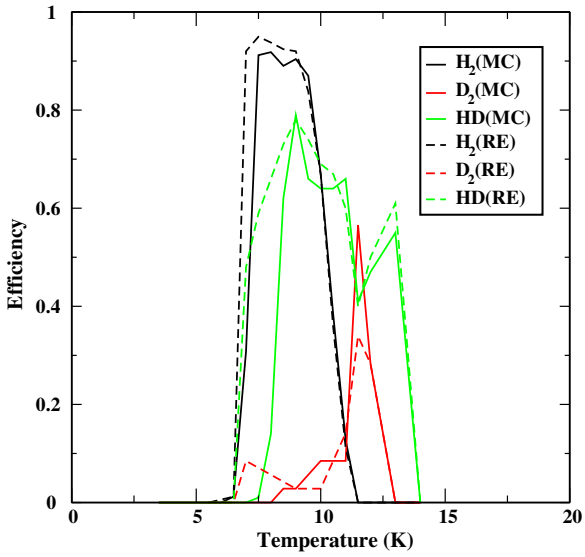

Fig. 3. Difference between cases when the spontaneous desorption factor is included (dashed line) and not included (solid line).

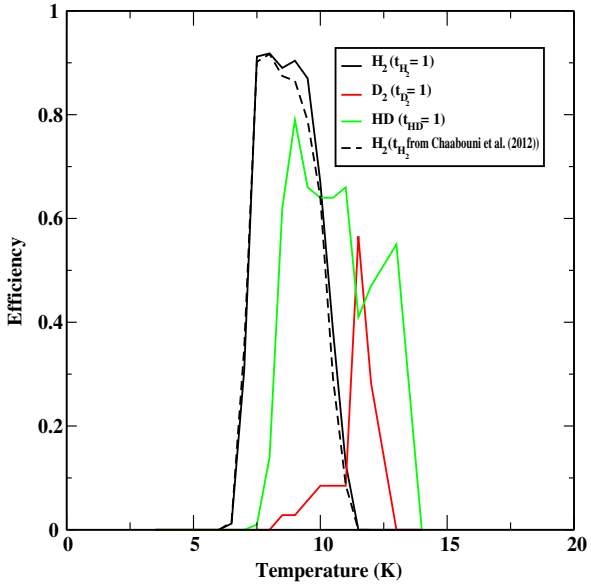

Fig. 4. Efficiency window of an olivine grain considering a sticking coefficient of 1 (solid lines) and the sticking coefficient from Chaabouni et al. (2012) (dashed line).

attains its maximum efficiency at 8.5 K, and the dashed line (considering spontaneous desorption) also attains a peak at 8.5 K. However, when the spontaneous desorption term is taken into account, *HD* starts being produced at somewhat lower temperatures. For example, a moderate efficiency at 7.5 K is achieved for the production of *HD* molecules when the spontaneous desorption term is considered, but at 7.5 K, the efficiency for the production of *HD* is ∼0 when the spontaneous desorption term is not considered. The reason for this result is that at low temperatures, thermal desorption time scales are considerably longer and the spontaneous desorption factor allows some species to release from the grain surface and populate the gas phase. Consequently, surface species begin to populate the gas phase at slightly lower temperatures when considering the spontaneous desorption factor.

Following Chaabouni et al. (2012), the sticking coefficients of *H* and *D* are calculated using Eq. (8). For a silicate grain, Chaabouni et al. (2012) considered a sticking parameter $(S_0) = 1$ for both *H* and *D* at $T_0 = 25$ K and 50 K. From Eq. (6), it is clear that the parameter is strongly dependent on temperature. In Fig. 4, a comparison between the consideration of a unity sticking coefficient (normal case and used for all the cases) and the consideration by Chaabouni et al. (2012) is shown for an olivine grain with $n_H = 10^2$ cm^{-3} and $r_D = 0.1$. Notably, in the regime of our simulation, when we are considering the sticking coefficients from Chaabouni et al. (2012), the productions of *HD* and D_2 are insignificant. Only a significant amount of H_2 is produced in this case. From 5–13 K, the sticking coefficient of *H*, as calculated from Chaabouni et al. (2012), varies in the range of 0.95–0.80. In the case of *D*, it varies in the range of 0.79–0.57.

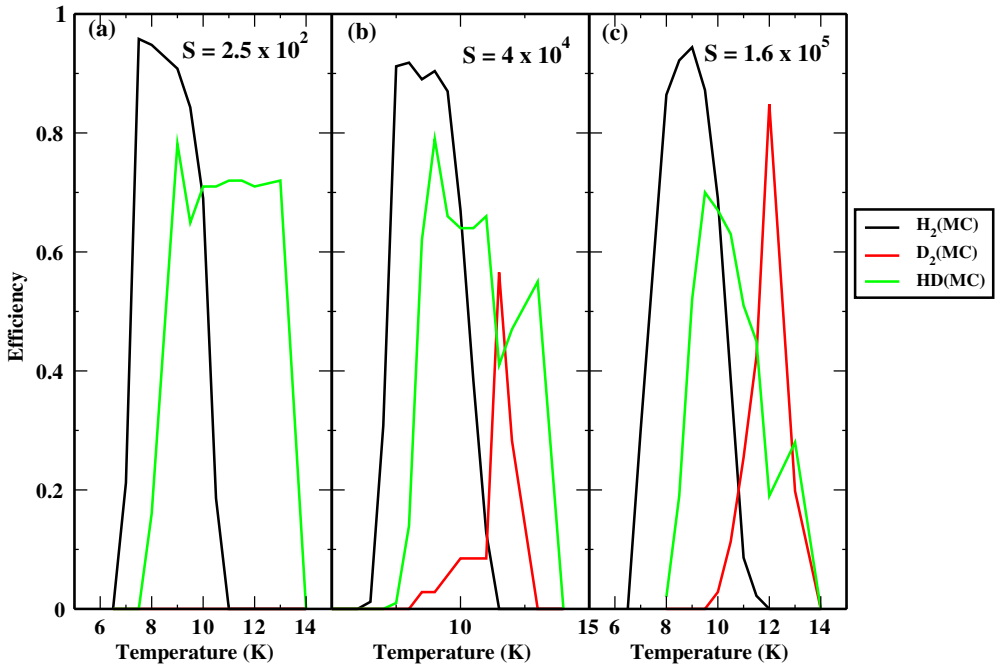

Fig. 5. Efficiency windows of an olivine grain with (a) 2.5×10^2, (b) 4×10^4 and (c) 1.6×10^5 number of sites.

Fig. 5a–c present efficiency windows for when the number of grain sites is varied. Here, we consider an olivine grain kept inside $n_H = 10^2$ cm^{-3} and $r_D = 0.1$. Fig. 5a–c show efficiency windows for an olivine grain with (a) 2.5×10^2 (Fig. 5a), (b) 4×10^4 (Fig. 5b) and (c) 1.6×10^5 (Fig. 5c) number of sites, respectively. Notably, for larger grains, all molecules are produced efficiently. For smaller-sized grains (with accretion limit grain, having $\sim 2.5 \times 10^2$ sites), D_2 is not produced. However, for the larger grains (1.6×10^5), D_2 is produced. From Fig. 5a–c, it is clear that as the grain size increases, the efficiency for the formation of D_2 increases.

In the previous discussion, it was indicated that the Monte Carlo method would provide a good estimation of the recombination efficiency and that the rate equation method would often over or under estimate the production rate. To overcome these discrepancies, Chakrabarti et al. (2006a,b) defined $A_x = a_x/S$, where A_x is the effective recombination rate of a surface species to recombine with another surface species and a_x is the hopping rate as defined previously. This is because in two dimensions, a species (random walker) needs some number of steps, which is linearly proportional to the number of distinct sites on the grain (Montroll and Weiss, 1965). If the grain has a total of S number of sites, then it should be proportional to S. In reality, S should be replaced by $S^{\alpha}(t)$, where $\alpha(t)$ depends on various physical and chemical properties of the grain (Chakrabarti et al., 2006a,b; Das et al., 2008a). In the rate equation, this linearity constant ($\alpha(t)$) is taken to be one, but in actuality, this may not be the case. The rate equation method is very popular because it is economical to perform using a computer, whereas the Monte Carlo method requires a long computational time even to handle a small chemical network. Chakrabarti et al. (2006a,b) first proposed the idea of calculating various values of $\alpha(t)$ to modify the rate equation in such a way that an educated estimation of a real scenario could be obtained using the simple rate equation method. Chakrabarti et al. (2006a,b) studied the formation of H_2 on interstellar grains and proposed values of $\alpha(t)$ under various physical conditions. Das et al. (2008a) studied the formation of water and methanol around a dense cloud using the same approach. In both cases, it was assumed that a steady state could be reached at $t \to \infty$ and that at steady state $\alpha(t) = \alpha$. Here, we consider diffuse cloud conditions, where H and D are randomly accreting and producing H_2, D_2 and HD. Due to the inherent nature of the diffuse cloud condition, the steady state condition may never be achieved (or achieved during a very late stage of evolution). Therefore, a steady state value of α could be misleading. Here, to avoid any discrepancies, we calculate a factor and name it the scaling factor (S_f), which is defined as follows:

$$S_f = \frac{\textit{Number of surface species X at time t by Monte Carlo method}}{\textit{Number of surface species X at time t by Rate equation method}}.$$

This factor defines the number of surface species as predicted by the Monte Carlo method with respect to that obtained using the rate equation method. Thus, after using the rate equation method, if we multiply the outcome by the scaling factor (S_f) defined above, we may obtain the results predicted by the Monte Carlo method. In Fig. 6, we show the variation in S_f for H_2, D_2 and HD for an olivine grain maintained at 9 K, $n_H = 10^4$ cm^{-3}, and $S = 4 \times 10^4$ with the number density of the cloud. For better illustration, $S_{f_{D_2}}$ is multiplied by 10 and $S_{f_{HD}}$ is multiplied by 5. Interestingly, as we increase the number density, S_f increases. The physical significance is that as we are going to a higher density regime, the grain surfaces are increasingly populated and the surface species could easily find its reactant partner to react with; thus, the production is enhanced.

For the low-density case, the production could be delayed due to the unavailability of a suitable reactant partner. Around the high-density region, the production efficiency increases and S_f increases. In Table 2, we present S_f for all species (H, D, H_2, D_2 and HD) for various sets of binding energies at temperatures where their production efficiency is maximum. For amorphous carbon grains, we provide the results for $T = 15$ K, and for intermediate energy values (set 3 energy values), $T = 11$ K. Similar trends could be observed for all sets of energies.

To determine the effects of the physical parameters on the formation of H_2, HD and D_2, we define another parameter β and name

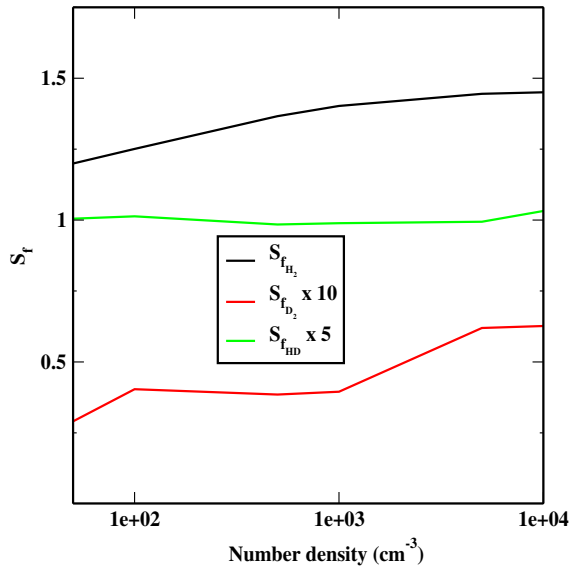

Fig. 6. Variation in S_f of H_2, D_2 and HD with number density of the cloud for an olivine grain maintained at 9 K. For clarity, $S_{f_{D_2}}$ and $S_{f_{HD}}$ are multiplied by 10 and 5, respectively.

it catalytic capability (β) by following Chakrabarti et al. (2006a,b) and Das et al. (2008a). This parameter measures the efficiency for the formation of H_2, HD and D_2 on a grain surface for a given pair of species residing on it. If δN_{D_2} is the number of D_2 formed in δt time, then the average rate of creation of D_2 per pair of deuterium atoms is given by

$$\langle A_{D1}(t)\rangle = \frac{1}{2N_D}\frac{\delta N_{D_2}}{\delta t}. \tag{15}$$

We identify the inverse of this rate as the average formation rate, and it is given by

$$T_f(t) = S^{\beta_{D_2}^{(t)}}/A_D. \tag{16}$$

Thus,

$$S^{\beta_{D_2}(t)} = A_D/\langle A_{D1}(t)\rangle. \tag{17}$$

This yields β as a function of time:

$$\beta_{D_2}(t) = log(A_D/\langle A_{D1}(t)\rangle)/log(S). \tag{18}$$

Similarly, for H_2 and HD,

$$\beta_{H_2}(t) = log(A_H/\langle A_{H1}(t)\rangle)/log(S), \tag{19}$$

$$\beta_{HD}(t) = log(A_{HD}/\langle A_{HD1}(t)\rangle)/log(S), \tag{20}$$

where

$$\langle A_{H1}(t)\rangle = \frac{1}{2N_H}\frac{\delta N_{H_2}}{\delta t}$$

and

$$\langle A_{HD1}(t)\rangle = \frac{1}{(N_H+N_D)}\frac{\delta N_{HD}}{\delta t}.$$

$\beta(t)$ is also a time-dependent parameter. At $t\to\infty$, $\beta(t)\to\beta$. As time evolves, grains are populated by the species. Because the surface coverage is increasing, the production should be faster due to the decrease in the reaction zone. However, there should also be a blocking effect (Das et al., 2008a); as a result of this effect, surface species could be locked for a period of time, which could in turn delay the production process. Therefore, the value of $\beta(t)$ also depends on the surface coverage. After some transient time steps, we obtain a steady state value of $\beta(t)$. Here, we are considering that at $t\to\infty$, $\beta(t)\to\beta$. In Fig. 7, we show the value of β with respect to the accretion rate per site. The values of β are calculated during the last few steps of our simulations ($\sim 10^8$ s). As expected, with increasing accretion rate, the surface coverage of species increases. In this situation, surface species need to travel a fewer number of steps to find one suitable reactant partner. A low value of β thus signifies a faster production rate, whereas a higher value represents a slower production rate.

In Fig. 8, a number of various surface species are shown with varying r_D. Observational evidence suggests that the elemental atomic D/H ratio (r_D) in the ISM would be $\sim 1.5\times 10^{-5}$ (Linsky et al., 1995). Here, we consider an olivine grain having 4×10^4 sites maintained at $T = 9$ K, $n_H = 10^2$ cm^{-3} and vary r_D from 10^{-5} to 0.1. Due to the randomness of the Monte Carlo method, we plot average numbers (average taken from the last few steps after $\sim 10^8$ s). For lower values of r_D, the production of D_2 is insignificant. The abundances of H and H_2 remain almost constant throughout the simulation range of r_D.

Table 2
Values of S_f for a wide parameter space.

Type of grain	Temperature (K)	Hydrogen number density (cm^{-3})	S_{f_H}	$S_{f_{H_2}}$	S_{f_D}	$S_{f_{D_2}}$	$S_{f_{HD}}$
Olivine	9	50	1.88	1.20	0.25	0.029	0.20
		100	1.84	1.25	0.24	0.04	0.20
		500	1.86	1.37	0.245	0.04	0.20
		1000	2.35	1.40	0.30	0.04	0.20
		5000	0.84	1.45	0.06	0.06	0.20
		10,000	1.21	1.45	0.09	0.06	0.21
Amorphous carbon	15	50	1.78	1.41	0.22	0.03	0.19
		100	1.79	1.41	0.22	0.03	0.19
		500	5.62	1.45	0.37	0.06	0.19
		1000	0.28	1.46	0.02	0.06	0.19
		5000	0.78	1.50	0.06	0.06	0.20
		10,000	0.63	1.50	0.045	0.07	0.20
Intermediate	14	50	1.96	0.91	0.29	0.04	0.20
		100	1.95	1.07	0.29	0.03	0.21
		500	1.93	1.30	0.27	0.04	0.21
		1000	1.99	1.34	0.28	0.04	0.21
		5000	1.53	1.38	1.15	0.05	0.203
		10,000	0.76	1.41	0.06	0.07	0.20

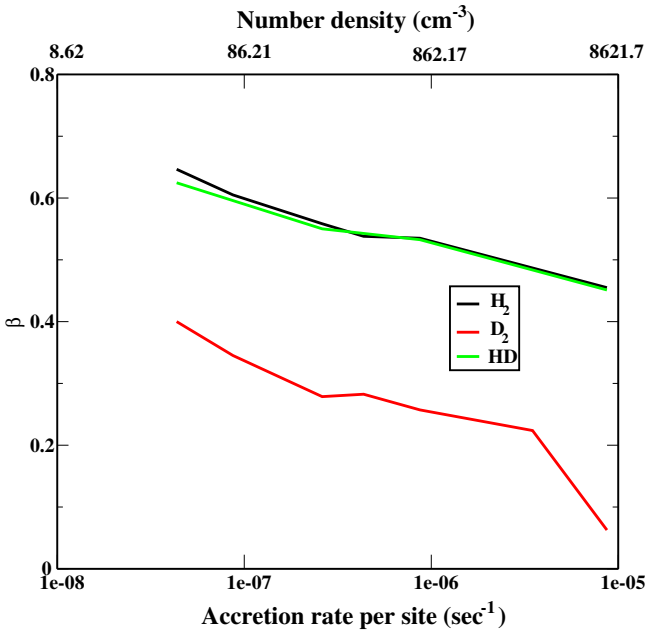

Fig. 7. Variation in β with the accretion rate per site (lower label of X axis) or number density of the cloud (upper label of the X axis).

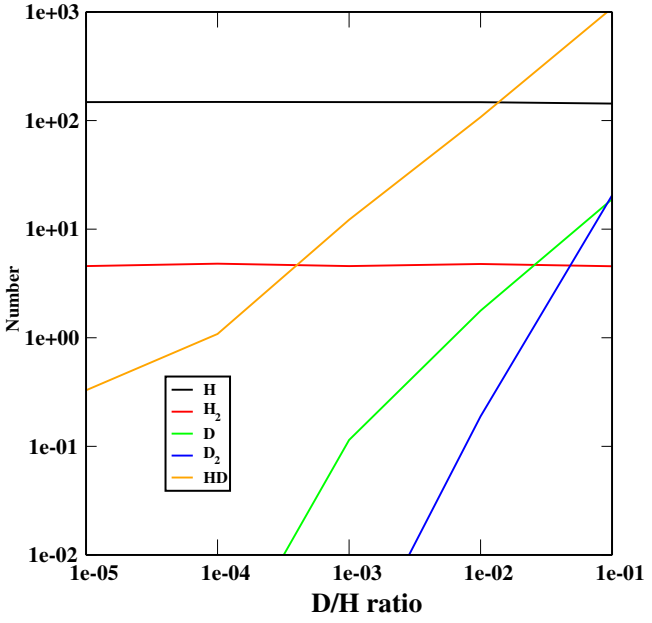

Fig. 8. Variation in the number of various surface species with varying r_D.

4. Conclusions

In this paper, we primarily focused on the production of H_2, D_2 and HD on grain surfaces. The highlights of our results are as follows:

- The production of these species is highly dependent on the types of grains (i.e., interaction energies). We conducted our simulations using three types of binding energies. For olivine grains, the efficiency window ranges from 8 to 14 K; for amorphous carbon grains, the window ranges from 11 to 22 K; and for binding energies as in LBH (set 3 energy values), this window is shifted to 11–19 K.
- We define a parameter S_f, which solely depends on various physical and chemical properties of interstellar grains. The rate equation method often over or under estimates the production efficiency. To obtain more accurate estimates of the production of these simple, yet most abundant, molecules in the ISM, this correction term should be considered in rectifying the results from the rate equation method. To broaden the application of our parameters, we provided a table (Table 2) with various values of S_f for a range of physical parameters.
- We computed another quantity β, named catalytic capacity, as used in earlier studies. This parameter shows a decreasing trend with increasing accretion rate. This implies that the production of surface species is increasingly favorable for the high accretion regime.
- Despite the low elemental abundance of atomic deuterium, several complex species are found to be heavily fractionated. Here, we vary the initial D/H ratio to determine the deuterium fractionation of the simplest, yet most abundant, species, namely, H_2. If we consider an elemental D/H ratio of 10^{-5} (Linsky et al., 1995) for a diffuse cloud where all H are in atomic form, the production of D_2 is found to be insignificant.

Acknowledgments

A.D., S.K.C. and D.S. would like to thank the ISRO respond project (Grant No. ISRO/RES/2/372/11-12) and DST project (Grant No. SB/S2/HEP-021/2013) for financial support. L.M. is grateful to a MoES project for financial support.

References

Biham, O., Furman, I., Pirronello, V., Vidali, G., 2001.
Buch, V., Zhang, Q., 1991. ApJ 379, 647.
Caselli, P., Stantcheva, T., Shalabiea, O., Shematovich, V.I., Herbst, E., 2002. P&SS 50, 1257.
Chaabouni, H., Bergeron, H., Baouche, S., Dulieu, F., Matar, E., Congiu, E., Gavilan, L., Lemaire, J.L., 2012. A&A 538A, 128.
Chakrabarti, S., Chakrabarti, S.K., 2000a. A&A 354, L6.
Chakrabarti, S.K., Chakrabarti, S., 2000b. Ind. J. Phys. 74B, 97.
Chakrabarti, S.K., Das, A., Acharyya, K., Chakrabarti, S., 2006a. A&A 457, 167.
Chakrabarti, S.K., Das, A., Acharyya, K., Chakrabarti, S., 2006b. BASI 34, 299.
Cuppen, H.M., Herbst, E., 2007. APJ 668, 294.
Das, A., Chakrabarti, S.K., 2011. MNRAS 418, 545.
Das, A., Chakrabarti, S.K., Acharyya, K., Chakrabarti, S., 2008a. NEWA 13, 457.
Das, A., Acharyya, K., Chakrabarti, S., Chakrabarti, S.K., 2008b. A & A 486, 209.
Das, A., Acharyya, K., Chakrabarti, S.K., 2010. MNRAS 409, 789.
Das, A., Majumdar, L., Chakrabarti, S.K., Chakrabarti, S., 2013a. NEWA 23, 118.
Das, A., Majumdar, L., Chakrabarti, S.K., Saha, R., Chakrabarti, S., 2013b. MNRAS 433, 3152.
Das, A., Majumdar, L., Chakrabarti, S.K., Sahu, D., 2015. NEWA 35, 53.
Gould, R.J., Salpeter, E.E., 1963. ApJ 138, 393.
Hasegawa, T., Herbst, E., Leung, C.M., 1992. APJ 82, 167.
Hollenbach, D., Werner, M.W., Salpeter, E.E., 1971. ApJ 163, 165.
Katz, N., Furmann, I., Biham, O., Pironello, V., Vidali, G., 1999. ApJ 522, 305.
Leith-Devlin, M.A., Williams, D.A., 1985. MNRAS 213, 295.
Linsky, J.L., Diplas, A., Wood, B.E., Brown, A., Ayres, T.R., Savage, B.D., 1995. ApJ 451 (335), B351.
Lipshtat, A., Biham, O., Herbst, E., 2004. MNRAS 348, 1055.
Majumdar, L., Das, A., Chakrabarti, S.K., Chakrabarti, S., 2012. Res. Astron. Astrophys. 12, 1613.
Majumdar, L., Das, A., Chakrabarti, S.K., Chakrabarti, S., 2013. New Astron. 20, 15.
Majumdar, L., Das, A., Chakrabarti, S.K., 2014a. A&A 562, A56.
Majumdar, L., Das, A., Chakrabarti, S.K., 2014b. ApJ 782, 73.
Matar, E., Bergeron, H., Dulieu, F., et al., 2010. J. Chem. Phys. 133, 104507.
Montroll, E.W., Weiss, G.H., 1965. J. Math. Phys. 6, 167.
Pirronello, V., Biham, O., Liu, C., Shena, L., Vidali, G., 1997. ApJ 483L, 131.
Pirronello, V., Liu, C., Riser, J.E., Vidali, G., 1999. A&A 344, 681.